Design of Experiments for the Stochastic Unit Commitment with Economic Dispatch Models

Nahal Sakhavand [a], Jay Rosenberger [a], Victoria Chen [a], Harsha Gangammanavar [b]

[a] Industrial, Manufacturing and Systems Engineering,
University of Texas at Arlington, Arlington, TX-76010 USA
[b] Department of Engineering Management, Information, and Systems,
Southern Methodist University, Dallas, TX-75275 USA

Abstract

We demonstrate a design and analysis of the computer experiments (DACE) approach to the stochastic unit commitment problem for power systems with significant renewable integration. For this purpose, we use a two-stage stochastic programming formulation of the stochastic unit commitment-economic dispatch problem. Typically, a sample average approximation of the true problem is solved using a cutting plane (such as the L-shaped method) or scenario decomposition (such as Progressive Hedging) algorithms. However, when the number of scenarios increases, these solution methods become computationally prohibitive. To address this challenge, we use a multivariate adaptive regression splines algorithm to approximate the second stage of the stochastic unit commitment-economic dispatch problem. We conduct the experiments on a modified IEEE118 test system and assess the quality of the solutions obtained from both the DACE and the L-shaped methods in a replicated procedure. The results obtained from this approach attest to the significant improvement in the computational performance of the DACE approach over the traditional L-shaped method.

Keywords: Unit commitment, economic dispatch, stochastic programming, design and analysis of computer experiments, multivariate adaptive regression splines, L-shaped method.

1 Introduction

Renewable energy is a critical resource in power system planning and operations, accounting for more than half of new U.S. power capacity installation [Perciasepe, 2017]. As the fastest-growing energy resource in the United States [C2ES, 2018], it offers several benefits for dispatch over conventional resources. The growth is attributed to consistently decreasing installation and operating costs over the past decade. The renewable portfolio standards set at the federal and state levels, have pushed the increase in the share of renewable generation in electricity portfolios [EIA, 2019]. Despite the economic and environmental benefits

of renewable resources, their integration on a large scale brings forth several challenges. For instance, the availability of intermittent renewable resources, namely solar and wind, depends on environmental conditions. Therefore, the power generation from these sources exhibits large fluctuations over short time periods. Due to their variability and intermittent nature, predicting generation amount from solar and wind resources is a demanding problem. Therefore, deterministic optimization frameworks that consider a single point forecast of uncertainty as input [Fallahi et al., 2019a,b, 2020] fail to capture the inherent stochasticity of the renewable resources. In this regard, stochastic programming (SP) approaches have been the subject of interest as they have proved to provide more realistic solutions while addressing the stochasticity of wind and solar [Atakan et al., 2021]. However, an SP approach exacerbates the computational challenges of optimizing the large-scale problems that arise in power systems planning and operations.

The unit commitment (UC) and the economic dispatch (ED) models are the main components of planning and operations in power systems. The day-ahead UC problem determines the generation and operating reserve schedules for the following day. It is a common practice to formulate the UC problems as mixed-integer linear programming (MILP) models. After the commitment decisions are set for the generators and the reserve requirements are met, the dispatch levels of the generators are established as the actual operating interval approaches by solving the ED problem. The dispatch levels are determined while maintaining a balance between the supply and demand and adhering to the physical constraints of the power systems components. ED models are typically formulated as linear programming problems [Osório et al., 2015].

The techniques used to solve stochastic UC (S-UC) problems have evolved since initially proposed by Wiebking [1977]. Decomposition techniques for S-UC were pioneered by Takriti et al. [1996] using scenario-based schemes such as the progressive hedging algorithm [Rockafellar and Wets, 1991] and later updated by Carpentier et al. [1996] with an augmented Lagrangian. Column generation algorithms, such as the work in Shiina and Birge [2004] have been considered for small-scale test instances with a small set of scenarios. Benders decomposition (BD) has been applied in a deterministic scheme [Wang et al., 2008] and for a robust formulation [Jiang et al., 2010, Bertsimas et al., 2012]. We refer the interested reader to Zheng et al. [2014] for a full review of the S-UC problems. Stochastic

ED (S-ED) problems have been frequently modeled using deterministic constraints [Liu and Zhong, 2010], a probabilistic approach [Hetzer et al., 2008], or decomposition methods such as stochastic decomposition (SD) [Gangammanavar et al., 2015].

Several articles leverage the decomposition-based SP framework to study the combined stochastic unit commitment-economic dispatch (S-UCED) problem ([e.g., Bouffard and Galiana, 2008, Wang et al., 2009, Papavasiliou and Oren, 2013]). In these works, the UC problem is included in the first stage to determine the commitment decisions. In the second stage, the ED problem is solved in response to a selected commitment decision and a realization of the uncertainty. In more recent research in Sakhavand and Gangammanavar [2020], a stochastic and simulation-based framework has been presented that uses the L-shaped method [Van Slyke and Wets, 1969] to solve the S-UCED problem.

The SP models for S-UCED aim to identify commitment decisions that are well-hedged against the uncertainty primarily due to demand and renewable generation. The S-UCED models use continuous random variables to model demand and renewable generation. Therefore, the resulting expectation-valued objective function involves high-dimensional integration. For computational tractability, a suitable representation of the underlying random variables is generated using sampling-based methods (e.g., Monte Carlo sampling) *a priori* to optimization. The continuous random variables are replaced by a finite and fixed sample of scenarios. The resulting optimization problem is referred to as the sample average approximation (SAA) [Shapiro et al., 2014]. Once the SAA problem is generated, decomposition (stage or scenario) methods can be employed to obtain a solution to the approximate problem. This approach has been used in several S-UC [Wang et al., 2011] and S-ED [Liu and Nair, 2015] problems.

Traditional cutting-plane algorithms, such as the L-shaped method, generate affine lower bounding functions or cuts to approximate the expected recourse function value. These cuts are added to the master problem as constraints. As the algorithm progresses, the size of the master problem grows linearly, and therefore, the computational difficulty grows significantly as the number of iterations increases. In contrast to the stage-decomposition approach of the L-shaped method, the progressive algorithm involves solving individual scenario problems, a primal aggregation, and a dual multiplier update steps. However, the performance of progressive hedging, particularly on S-UC problem, is known to be sensitive

to the parameters used in the dual multiplier update step [Cheung et al., 2015]. In any case, both of these decomposition methods are applicable only when the underlying support is finite or when the SAA problem is being solved. Given the notoriously challenging NP-hard nature of the stochastic MILP problems, solving realistically large-scale S-UCED problems remains a challenge.

An alternative approach to ease the computational effort is to apply design and analysis of computer experiments (DACE). The DACE approach was first proposed by Sacks et al. [1989] and later suggested by Chen [2001] for SP models to accelerate the convergence over the traditional methods. The use of the DACE approach has shown to be appealing in solving 2-SP models such as the work studied in Pilla et al. [2008, 2012]. This approach exploits a metamodel as a surrogate to approximate the expectation-valued objective function of the SP model given the design parameters. To construct the metamodel, one must implement two primary steps: (1) use an experimental design to select a set of sample points that cover the parameters' feasible region known as the design space; and (2) fit a statistical model to the output of the observed sample points [Lin et al., 2001]. The common design of experiments techniques that can be used to fill the design space include Latin hypercubes, orthogonal arrays, and number-theoretic methods. The Latin hypercube design was first proposed in Patterson [1954]. Later, McKay et al. [2000] extended the design for the case of a continuous range of each variable using a uniform distribution over each interval. As for the statistical modeling step, common statistical methods include but are not limited to regression trees and multivariate adaptive regression splines (MARS). MARS as a non-parametric algorithm was first proposed by Friedman [1991], which creates a piecewise linear model to discover the relationships between a response value and the predictors that are additive or involve predictor interactions effects. For our practical purposes, we use the latter to construct our metamodel along with the Latin hypercube sampling (LHS) method. For a full review on selecting an appropriate experimental design and statistical model for constructing the metamodel, we refer the interested reader to Chen et al. [2006]. It is worthwhile to note that unlike the decomposition methods (L-shaped and progressive hedging), the DACE approach does not rely on the finiteness of the underlying stochastic process. In this regard, DACE approaches may aim to solve problems that do not necessarily approximate the uncertainty with a finite discrete support set.

Compared with existing literature, the main contributions made in this research are as follows:

- We present a DACE-based approach that uses a metamodel to approximate the expected recourse function in the two-stage S-UCED model. The first stage of the formulation corresponds to the unit commitment. We determine these decisions before observing a realization of the uncertainty in renewable generation. Subsequently, we model the dispatch procedure in the second stage. The second stage responds to a fixed commitment decision and a realization of the uncertainty in renewable generation. To the best of our knowledge, our work provides the first application of the DACE approach to the S-UCED problem. This approach is based on the idea from Chen [2001] and provides computationally tractable solutions in a statistics-based framework. Moreover, we customize our approach to take advantage of the special structure of the unit commitment problem in the first stage to generate the design of experiments. The relationship between commitment decisions favors developing special features on how long the generators operate and their status in certain periods. We utilize these features to predict the second-stage recourse function value.

- We fit our statistical model for the expected recourse function using MARS. This model controls the number of subproblems to solve in the second stage, which is impossible to track in traditional cutting-plane algorithms. In addition, it develops an understanding of the relationship between the recourse function and the input space. In particular, our MARS model provides information on which generators have the most impact on the potential operating costs.

- We compare our results with the well-recognized L-shaped method. Using the DACE approach reveals a significant reduction in the computing time over the traditional L-shaped method on a standard test instance with a large set of scenarios. This allows the system operators to make planning and operational decisions within the tight time frame considered in the electricity market.

The rest of the paper is organized as follows. In Section 2, we present the UC and ED models as well as a detailed and general framework of the S-UCED model. Section 3 provides a comprehensive description of the DACE-based approach used to solve the

problem followed by presenting the numerical results in Section 4. Finally, we conclude the paper in Section 5 with a brief discussion on future trends.

2 Problem Formulation

In this section, we present the two-stage SP formulation for the combined S-UCED problem. We first present the two components, viz., UC and ED, and then introduce the combined form. For our purposes, we consider a power system with buses (nodes) denoted by $\mathcal{B}$ and transmission lines denoted by $\mathcal{L}$. We denote the subset of nodes that connect to loads by $\mathcal{D}$. Finally, we denote by $\mathcal{G}$ and $\mathcal{R}$ the sets of conventional and renewable generators, respectively. We use $\mathcal{T}$ to denote the set of decision epochs within the problem horizon.

2.1 Unit Commitment

The UC problem formulation is based on Atakan et al. [2017]. For a generator $g \in \mathcal{G}$, we define the state decision variable $x_{g,t}$. It takes a value of one if the generator remains operational in time period $t \in \mathcal{T}$, otherwise it takes a value of zero. Binary variables $s_{g,t}$ and $z_{g,t}$ denote the generator start up and shut down variables, respectively. These variables take a value of one if the generator is switched on (or off) in time period $t \in \mathcal{T}$, and zero otherwise. Using these variables, it is possible represent the transition of the generator state in one period to the next on a network. With this perspective, the state transition is captured by the following flow balance equation:

$$s_{g,t-1} + x_{g,t-1} = z_{g,t} + x_{g,t} \qquad \forall g \in \mathcal{G},\ t \in \mathcal{T}. \tag{1}$$

It is worthwhile to notice that the above relation ensures that the variables $x_{g,t}, s_{g,t}$ and $z_{g,t}$ cannot simultaneously be one or zero.

The common constraints incorporated in the UC problem capture the restrictions imposed by the underlying physics. The minimum downtime/uptime constraints enforce the

requirement for a unit to stay on/off for a minimum amount of time. These are given by

$$\sum_{i=t-UT_g+1}^{t-1} s_{g,i} \leq x_{g,t} \qquad \forall g \in \mathcal{G},\ t \in \mathcal{T}, \tag{2a}$$

$$\sum_{i=t-DT_g}^{t} s_{g,i} \leq 1 - x_{g,t-DT_g} \qquad \forall g \in \mathcal{G},\ t \in \mathcal{T}. \tag{2b}$$

Here, UT_g and DT_g are the minimum uptime and downtime limits, respectively, that are characteristic of a generator g. Constraint (2a) ensures that a remain-on generator could have been turned on at most once in the previous $UT_g - 1$ time periods. Similarly, constraint (2b) suggests that if a generator remains operational, it cannot be switched on again in the current time period t or the next DT_g time periods.

We define two different variables to capture the generation amount in the UC problem. The first variable, denoted by $G'_{g,t}$, captures the amount of generation beyond the minimum capacity of an operational generator denoted by $\underline{C}_g$. Since we consider a stochastic setting, we may revise the generation amount determined in the UC stage during dispatch. Furthermore, the committed generators can also act as spinning operating reserves to cover the discrepancy between the forecast and actual renewable generation. The second variable captures the maximum amount of generation that a generator can produce to cover for any shortfall in renewable generation. We denote this variable as $\overline{G}_{g,t}$. Typically, the power system operators require a certain minimum amount of spinning reserves to be committed in the UC problem. We denote the required reserve amounts by ρ_t. These maximum generation decision variable must satisfy

$$\sum_{g \in \mathcal{G}} \overline{G}_{g,t} \geq \left(\sum_{i \in \mathcal{D}} D_{i,t} - \sum_{i \in \mathcal{R}} \breve{G}_{i,t} \right) + \rho_t \qquad \forall t \in \mathcal{T} \tag{3}$$

where $\breve{G}_{i,t}$ is the forecast of renewable generation from $i \in \mathcal{R}$ and $D_{i,t}$ is the demand at node $i \in \mathcal{D}$. The parenthetical term on the right-hand of the inequality (3) is often referred to as the net demand that represents the amount the generation expected to be met by the conventional generation resources.

The maximum generation $\overline{G}_{g,t}$ and the generation amount $G'_{g,t}$ are related to the on and off status of the generator through the following constraints:

$$\overline{G}_{g,t} \geq G'_{g,t} + \underline{C}_g(s_{g,t} + x_{g,t}) \qquad \forall g \in \mathcal{G},\ t \in \mathcal{T}, \tag{4a}$$

$$\overline{G}_{g,t} \leq \overline{C}_g(s_{g,t} + x_{g,t}) + (\underline{S}_g - \overline{C}_g) z_{g,t+1} \qquad \forall g \in \mathcal{G},\ t \in \mathcal{T}. \tag{4b}$$

In the above, $\overline{C}_g$ is the maximum generation capacity when g is operational, respectively. Additionally, $\overline{S}_g$ and $\underline{S}_g$, respectively denote the minimum capacity that a generator must meet upon startup and before it is shutdown. The following demand constraints ensure the expected net demand is met by the committed conventional generators and is presented as follows:

$$\sum_{g\in\mathcal{G}}(G'_{g,t}+\underline{C}_g(s_{g,t}+x_{g,t}))\geq\left(\sum_{i\in\mathcal{D}}D_{i,t}-\sum_{i\in\mathcal{R}}\breve{G}_{i,t}\right)\qquad\forall t\in\mathcal{T}. \tag{5}$$

Finally, the ramping constraints relate the generation amounts from one time period to the next for all the committed conventional generators. These constraints are given by:

$$\overline{G}_{g,t}-G'_{g,t-1}\leq\overline{S}_g s_{g,t}+(\overline{R}_g+\underline{C}_g)x_{g,t}\qquad\forall g\in\mathcal{G},\ t\in\mathcal{T}, \tag{6a}$$

$$G'_{g,t-1}-G'_{g,t}\leq(\underline{S}_g-\underline{C}_g)z_{g,t}+\underline{R}_g x_{g,t}\qquad\forall g\in\mathcal{G},\ t\in\mathcal{T}, \tag{6b}$$

where $\overline{R}_g$ and $\underline{R}_g$ are the ramp up and ramp down limits. Constraint (6a) ensures that the increase in the generation output of the remain-on generator is limited by $\overline{R}_g$. On the other hand, the generation of a generator that is switched on is bounded by $\overline{S}_g$. The constraint (6b) ensures that the decrease in generation of a remain-on generator is limited by the ramp down limit $\underline{R}_g$. The constraint also ensures that the generator that is switched off in time period t does not generate more than $\underline{S}_g$ in the previous time period.

2.2 Economic Dispatch

In the ED model, the system responds to a realized demand and renewable generation outcome by adapting actual generation levels of all generators committed in the UC solution. While the UC model ensures that the generation and demand quantities are balanced at a system-level, the ED problem incorporates a more detailed representation of the power network. For this purpose, we additionally define variables for power flow on a line $(i,j)\in\mathcal{L}$, denoted $p_{(i,j),t}$, and phase angle $\theta_{i,t}$ for a node $i\in\mathcal{B}$ for all time periods $t\in\mathcal{T}$. In this stage, the generation resources are adjusted to the prevailing conditions, which may be different from the forecasts used in the day-ahead UC stage. The ED model that we present here is based on Gangammanavar et al. [2015].

For generator g at each time period t, we assume that the hour-ahead generation cost $v_{g,t}$ is a piece-wise linear convex function of the dispatch amounts. Variables for the load

curtailment at demand node i, r^{ls}_{it}, and generation curtailment at generator g, r^{gs}_{gt}, at time t are other components of the objective function given below.

$$\min \quad \sum_{t\in\mathcal{T}}\left(\sum_{g\in\mathcal{G}} v_{g,t} + \sum_{g\in\mathcal{G}\cup\mathcal{R}} d^{gs}_g r^{gs}_{g,t} + \sum_{i\in\mathcal{D}} d^{ls}_i r^{ls}_{i,t}\right). \tag{7}$$

Here, d^{gs}_g and d^{ls}_i are the shedding penalties for generator g and load at node i.

Since only committed generators are capable of generating within their capacities in the ED problem, they must satisfy the following constraints:

$$\underline{C}_g(x_{g,t}+s_{g,t}) \le G_{g,t} \le \overline{C}_g(x_{g,t}+s_{g,t}) \qquad \forall g\in\mathcal{G},\ t\in\mathcal{T}. \tag{8}$$

Similar to the UC model, ramping constrains are imposed on generation as follows:

$$G_{g,t} - G_{g,t-1} \le \overline{S}_g s_{g,t} + \overline{R}_g x_{g,t} \qquad \forall g\in\mathcal{G},\ t\in\mathcal{T}, \tag{9a}$$

$$G_{g,t-1} - G_{g,t} \le \underline{S} z_{g,t} + \underline{R}_g x_{g,t} \qquad \forall g\in\mathcal{G},\ t\in\mathcal{T}. \tag{9b}$$

Notice that the variable $G_{g,t}$ in ED is analogous to $G'_{g,t}+\underline{C}_g$ in the UC model.

At each bus in the network, flow balance equations guarantee that the demand is satisfied through the available generation or through power flows on lines connected to the bus. The flow balance equations are presented below.

$$\sum_{j:(j,i)\in\mathcal{L}} p_{ji,t} - \sum_{j:(i,j)\in\mathcal{L}} p_{ij,t} + \sum_{j\in\mathcal{G}_i}\left(G_{j,t} - r^{gs}_{j,t}\right) + \sum_{j\in\mathcal{R}_i}\left(G_{j,t}(\tilde{\xi}) - r^{gs}_{j,t}\right) = \sum_{j\in\mathcal{D}_i}\left(D_{j,t} - r^{ls}_{j,t}\right) \quad \forall i\in\mathcal{B},\ t\in\mathcal{T}. \tag{10}$$

In the above, we use $\mathcal{G}_i \subseteq \mathcal{G}$ to denote the subset of generators that are connected to bus $i\in\mathcal{B}$. Similarly, $\mathcal{D}_i\subseteq\mathcal{D}$ and $\mathcal{R}_i\subseteq\mathcal{R}$ denote the subset of loads and renewable generators connected to bus i, respectively. In our model, we allow the excess generation (from both conventional and renewable resources) to be shed and demand to be curtailed. The amount of generation shed is captured by $r^{gs}_{g,t}$ and demand curtailment by $r^{ls}_{j,t}$.

The power flow on a transmission line $(i,j)\in\mathcal{L}$ depends on the voltage set at the connected buses i and j. These quantities (power flows and voltages) are complex number that are connected through nonlinear relationships. In practice, a linear approximation that ignores the imaginary (reactive) part of power flow and line losses is commonly employed.

We adopt such a linear or direct current (DC) approximation of the power flows. These are given by

$$p_{ij,t} = \frac{V_i V_j}{X_{ij}}(\theta_{i,t} - \theta_{j,t}) \quad \forall (i,j) \in \mathcal{L}, t \in \mathcal{T}, \tag{11}$$

where V_i is the voltage magnitude at bus i and X_{ij} is the reactance of line (i,j).

The power flows, the voltage angles, the generation shedding, and load curtailment variables are bounded as follows:

$$p_{ij}^{min} \leq p_{ij,t} \leq p_{ij}^{max} \qquad \forall (i,j) \in \mathcal{L},\ t \in \mathcal{T}, \tag{12a}$$

$$\theta_i^{min} \leq \theta_{i,t} \leq \theta_i^{max} \qquad \forall i \in \mathcal{B}, t \in \mathcal{T}, \tag{12b}$$

$$0 \leq r_{i,t}^{ls} \leq D_{i,t} \qquad \forall i \in \mathcal{D},\ t \in \mathcal{T}, \tag{12c}$$

$$0 \leq r_{i,t}^{gs} \leq G_{i,t} \qquad \forall i \in \mathcal{G} \cup \mathcal{R},\ t \in \mathcal{T}, \tag{12d}$$

where θ^{min} and θ^{max} are the voltage angle limits and p^{min} and p^{max} are line capacity limits.

The generation cost is a piecewise affine function of the generation amounts. If there are $\kappa_g^{\max}$ pieces for a generator $g \in \mathcal{G}$ then we denote by c_g^κ the coefficients and γ_g^κ the breakpoints an individual piece $\kappa = 1, \ldots, \kappa_g^{\max}$. The coefficients satisfy $c_g^1 \leq c_g^2 \leq \ldots \leq c_g^{\kappa^{\max}}$. The aggregate cost of generating $G_{g.t}$ units is represented by the function $\widehat{Q}(G_{g,t})$. These costs are incorporated in the model by using auxiliary variables $v_{g,t}$. With these definitions, we enforce the piecewise generation costs using the following constraints:

$$v_{g,t} \geq c_g^\kappa (G_{g,t} - \gamma_g^{\kappa-1}) + \widehat{Q}_g(\gamma_g^{\kappa-1}) - \widehat{Q}(\underline{C}_g) \quad \forall g \in \mathcal{G},\ t \in \mathcal{T}, \quad \kappa = 1, \ldots, \kappa^{max}. \tag{13}$$

The above ensures that the unit generation cost within interval $[\gamma_g^\kappa, \gamma_g^{\kappa+1}]$ is c_g^κ.

2.3 Decomposed Multi-period Two-stage S-UCED Model

Using the UC and ED model components introduced in the previous subsection, we next present the decomposed multi period two-stage S-UCED models. In this model the UC problem constitutes the first stage and ED problem is the second stage. The two-stage S-UCED is given as

$$\min \quad \sum_{t \in \mathcal{T}} \left(\sum_{g \in \mathcal{G}} \left(f_{g,t}^{SU} s_{g,t} + f_{g,t}^{SD} z_{g,t} + \widehat{Q}(\underline{C}_g)(s_{g,t} + x_{g,t}) \right) \right) + \mathbb{E}\{h(x,s,z,\tilde{\xi})\} \tag{UC}$$

$$\text{s.t } (1) - (6),\ (x,s,z) \in \{0,1\}^{3|\mathcal{G}||\mathcal{T}|},\ (G', \overline{G}) \geq 0,$$

where,

$$h(x,s,z,\xi) = \min \quad \sum_{t\in\mathcal{T}}\left(\sum_{g\in\mathcal{G}} v_{g,t} + \sum_{g\in\mathcal{G}\cup\mathcal{R}} d_g^{gs} r_{g,t}^{gs} + \sum_{i\in\mathcal{D}} d_i^{ls} r_{i,t}^{ls}\right) \qquad \text{(ED)}$$

$$\text{s.t } (8)-(13).$$

For the purpose of illustrating our DACE solution, we use a following general two-stage SP form with a mixed-binary first stage and a continuous recourse.

$$\min \ f(\mathbf{u},\mathbf{v}) := c(\mathbf{u},\mathbf{v}) + \mathbb{E}\{Q(\mathbf{u},\tilde{\xi})\} \qquad \text{(14a)}$$

$$\text{s.t } (\mathbf{u},\mathbf{v}) \in \mathcal{V} := \{(\mathbf{u},\mathbf{v}) \mid A[\mathbf{u};\mathbf{v}] = b\} \subseteq \mathbb{B}^{m_1} \times \mathbb{R}_+^{n_1},$$

where the uncertain demand and renewable generation is represented by $\tilde{\xi}$, and the recourse function is the optimal value of the following problem:

$$Q(\mathbf{u},\xi) = \min \ d(\mathbf{y},\xi) \qquad \text{(14b)}$$

$$\text{s.t } W\mathbf{y} = r(\xi) - T\mathbf{u}, \ \mathbf{y} \in \mathbb{R}_+^{n_2}.$$

In the above general form, we distinguish between the binary commitment decision variables, $\mathbf{u}$, and continuous decision variables captured by $\mathbf{v}$. The continuous decision variables, denoted by $\mathbf{y}$, are determined adaptively after the realization ξ is revealed. We assume that the random variable $\tilde{\xi}$ is defined over the probability space $(\Xi, \mathcal{F}, P)$, where Ξ is the sample space and corresponds to the set of random variable outcomes, $\mathcal{F}$ is the set of outcomes in the sample space, and P is the probability measure function. Notice that the two-stage SP form of S-UCED satisfies fixed and relatively complete recourse. The former implies that the recourse matrix W is deterministic. The later implies that the second-stage program is feasible for any first-stage decision $(\mathbf{u},\mathbf{v}) \in \mathcal{V}$ and observation $\xi \in \Xi$. The feasibility of the ED problem is attributed to the ability to shed excess generation and curtail load (see (10) and the subsequent discussion). In S-UCED, notice that only the right-hand side of the second-stage constraints have random elements (random demand and renewable generation).

3 The DACE Approach

Figure 1a illustrates the DACE process for two-stage stochastic programming problems, as proposed in Chen [2001], and Figure 1b shows an adapted version of this approach applied

to the model in (14). The input and output of the algorithm in the DACE approach are generally assumed to be numerical. In our case, the region of study in the first stage (14a) is a binary space. To tackle the intractability of modeling over a high-dimensional binary space, we introduce a numerical feature space to represent the commitment decisions and allow an approximation using the MARS statistical model. Further, the design of experiments (DoE) ideally desires an orthogonal space, which corresponds to no multicollinearity in the feature space to enable causal modeling. Because the constraints in (14) directly impose collinear structure, DoE is conducted over a more controllable space from which the commitment decisions are derived and then used as input to the second stage optimization problem to obtain feasible recourse values for Step 3 in Figure 1b. The resulting MARS statistical model that estimates the expected recourse function can then be globally optimized.

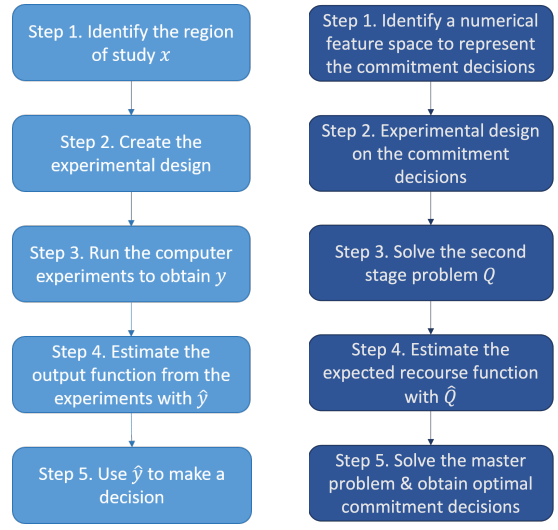

(a) DACE approach procedure

(b) DACE approach for S-UCED

Figure 1: The detailed steps of the DACE approach

3.1 Defining the Feature Space

In this section, we describe Step 1 of the flowchart in Figure 1b. For the DACE process, the feature space must be appropriately specified to enable a good estimate of the recourse function in Step 4. In our case, the most straightforward feature space consists

of (x_{gt}, s_{gt}, z_{gt}) for every unit g at time period t that satisfies the first stage constraints of (14a). However, there are three concerns with employing the commitment decisions directly as the DACE feature space. First, the original binary space is high-dimensional, involving $3|\mathcal{G}||\mathcal{T}|$ variables. Second, these features are binary, and while it is possible to conduct DoE for a binary feature space, this will not enable a good approximation in Step 4. Finally, as previously mentioned, the commitment decisions are collinear variables. This is specifically noticeable in the state transition constraints (1) that link these variables and the minimum downtime and uptime constraints (2). The inevitable multicollinearity of such a large number of predictors renders a good DoE impossible and would result in an unstable approximation model in Step 4 [Kutner et al., 2004, Ariyajunya et al., 2020]. To overcome these challenges, we partition the day into time intervals denoted by $\mathcal{I}$. For each interval $i \in \mathcal{I}$, we use $\mathcal{T}_i$ to denote its time periods. For any time interval i, we define a numerical input space by introducing nonnegative integer features l_{gi} that capture the number of time periods at which unit g remains on within that interval. The new *commitment linking* feature space has $|\mathcal{G}||\mathcal{I}|$ variables. These variables are mapped to the first-stage variable space through the following constraint in the optimization model.

$$l_{gi} = \sum_{t \in \mathcal{T}_i} x_{g,t} \qquad \forall g \in \mathcal{G} \qquad \forall i \in \mathcal{I}. \tag{15}$$

3.2 Generating the Experimental Design

This section details Step 2 of the flowchart in Figure 1b. In general, DoE requires specification of the range on the feature space over which DoE is constructed. Given our feature space defined by the commitment linking variables l_{gi}, the challenge here is identifying a reasonable range. Instead of directly constructing DoE over the l_{gi} variables, the available generator data can be utilized to identify the consecutive periods of uptime and downtime. DoE is then used to sample hypothetical sequences of uptime and downtime for each generator, and the commitment linking variables l_{gi} can then be calculated based on these sequences. Let the minimum length of consecutive periods required for generator g to remain on and off be MinUT_g and MinDT_g, respectively. This definition is synonymous with the definition of minimum uptime and downtime discussed in the UC problem. Subsequently, let the maximum number of consecutive time periods that generator g requires

to remain on and off be MaxUT_g and MaxDT_g, respectively over the course of the 24-hour horizon.

For each generator g, we use MinUT_g and MinDT_g data to identify the maximum number of changes in the commitment status of each generator from remaining on to remaining off and vice-versa. For instance, if MinUT_g is two hours and MinDT_g is one hour, then there can be at most eight status changes in a 24-hour horizon, with at most four switch-on or switch-off changes. We denote by $\Omega_g$to be the maximum number of switch on or switch off status changes. Furthermore, we use $\overline{\omega}_g$ and $\underline{\omega}_g$ to denote random variables that correspond to the uptime and downtime, respectively. The random variable $\overline{\omega}_g$ is defined over the support $[\text{MinUT}_g, \text{MaxUT}_g]$. Similarly, $\underline{\omega}_g$ is defined over the support $[\text{MinDT}_g, \text{MaxDT}_g]$. Using these random variables, we can generate a sequence of $2 \times \Omega_g$.

We simulate Ω_g outcomes of $\underline{\omega}_g$ and $\overline{\omega}_g$, and arrange them in an alternating order. We refer to the resulting sequence as an *observation*. If $\{\underline{\omega}_{g,1}, \underline{\omega}_{g,2}, \ldots, \underline{\omega}_{g,\Omega_g}\}$ are the simulated outcomes of $\underline{\omega}_g$ and $\{\overline{\omega}_{g,1}, \overline{\omega}_{g,2}, \ldots, \overline{\omega}_{g,\Omega_g}\}$ are the outcomes of $\overline{\omega}_g$, then an observation will have the following form:

$$\mathcal{O}_g = (\underline{\omega}_{g,1}, \overline{\omega}_{g,1}, \underline{\omega}_{g,2}, \overline{\omega}_{g,2}, \ldots, \underline{\omega}_{g,\Omega_g}, \overline{\omega}_{g,\Omega_g}).$$

Notice that an observation is a realization of duration of uptime and downtime sequences for a generator.

Given an observation, we can construct the features (UC decision vector) of $(x_{g,t}, s_{g,t}, z_{g,t})$ for the entire 24-hour horizon. If the generator remains on during a current time period t, and is off in the next time period $t+1$, the unit must have been switched off at the beginning

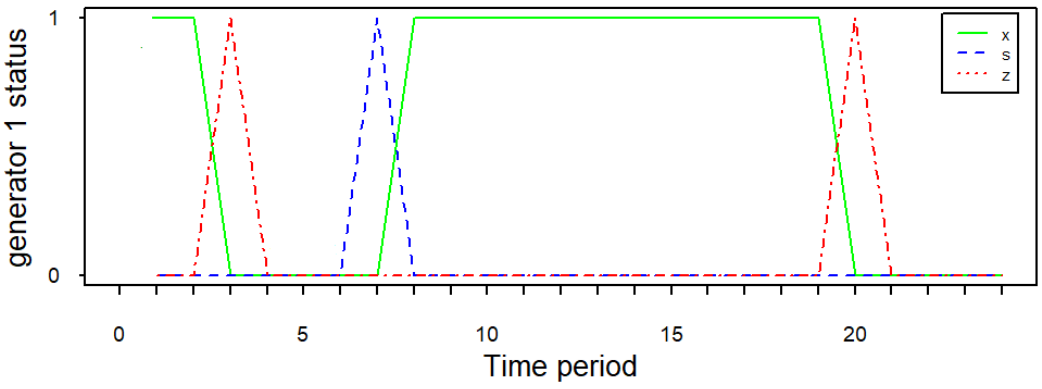

Figure 2: Commitment status for generator 1 in a 24-hour period

of period $t+1$; i.e., $z_{g,t+1} = 1$. We can obtain the switching on of the unit g denoted by s_{gt} in a similar manner. We capture this construction using a mapping ϕ which we illustrate through an example. Consider the following observation $\mathcal{O}_g = (2, 5, 12, 5, 0, 0)$. The feature values are shown in Figure 2. Notice since $\overline{\omega}_{g,1} = 2$, the generator remains on for the first two time periods and it's switched off in the third time period; therefore, $z_{g,3} = 1$. Since $\underline{\omega}_{g,1} = 5$, the generator remains off until $t = 7$. It is then switched on resulting in $s_{g,7} = 1$.

We use Latin hypercube sampling (LHS) design [McKay et al., 2000] to generate a set of N observations. An experimental design is a matrix, with columns representing the different dimensions of the design space and the rows representing the realized sequences. Here, the dimension of the design space is $2\sum_g \Omega_g$ to accommodate both the observations for all the generators. For our LHS design, we generated N observations (N rows in the design matrix). The experimental design is standardized to a range of values between 0 and 1. For a column representing uptime for a specific generator, the value is scaled to its support, i.e., $[\text{MinUT}_g, \text{MaxUT}_g]$. Similarly, if a column represents downtime, the value is scaled to its support $[\text{MinDT}_g, \text{MaxDT}_g]$. Since we consider one-hour time steps, we round the resulting realization to the nearest integer. We summarize these steps in Algorithm 1.

Algorithm 1: Experimental design with LHS

Input: Generator data $\text{MinUT}_g, \text{MaxUT}_g, \text{MinDT}_g, \text{MaxDT}_g$, Ω_g for $\{g \in \mathcal{G}\}$; the number of observations, N.

for $\{g \in \mathcal{G}\}$ **do**

Step 1. Construct a LHS design with dimension $2\Omega_g$; with interval [MinUT_g, MaxUT_g], [MinDT_g,MaxDT_g] for random variables $\overline{\omega}_g$ and $\underline{\omega}_g$, respectively; N discritizations (levels).

for $n = 1, ..., N$ **do**

Step 2. Construct observations $\mathcal{O}_g^n$.

Step 3. Compute $\phi(\mathcal{O}_g^n) = (x_{gt}^n, s_{gt}^n, z_{gt}^n)$.

Output: Features (UC desicions) for all generators and time periods.

It is necessary that the final sampled set of DoE points lie within the feasible region of the first stage (14a). Namely, DoE points generated in Step 1 of Algorithm 1 should result in enough operational (remain-on) time periods for each unit to meet the demand and operating reserve requirements in the UC problem. In order to ensure that DoE

points satisfy these constraints, we solve the following mean value problem which provides optimistic solutions for the (14).

$$\min_{(\mathbf{u},\mathbf{v})\in\mathcal{V}} f(\mathbf{u},\mathbf{v}) := c^\top[\mathbf{u};\mathbf{v}] + Q(\mathbf{u},\overline{\xi}). \tag{16}$$

The optimal objective function value of the mean value problem provides a lower bound for the expected recourse value. Hence, we use the optimal commitment solutions of (16) as a baseline for our DoE procedure to identify the conventional generators that always remain on (i.e., $x_{g,t} = 1$ for $t \in \mathcal{T}$). These values are fixed a priori to the DoE. Additional approaches to address this challenge are worth a complete discussion and are recommended as future work.

3.3 Approximating the Recourse Function

This section describes Step 3 and 4 of the DACE flowchart in Figure 1b. Once we simulate the design points and map them to the commitment decision space of $(\mathbf{x}, \mathbf{s}, \mathbf{z})$ in Step 2, we solve the second stage problem (14b) to obtain the corresponding recourse values Q for each observation n in Step 3.

To approximate the second stage problem, we use the MARS approximation to fit to the recourse values in Step 4. The MARS model represents the relationships between the expected recourse function and the commitment decisions. This statistical model is a weighted sum of basis functions denoted by $B_j(\mathbf{l})$ for the input variable $\mathbf{l}$ and can be of a form of a constant, a univariate hinge function modeled as

$$b(\mathbf{l}) = \max\{0, \pm(l_{gi} - k)\}, \tag{17}$$

or a product of two or more univariate functions. Here, k is the knot at which the function bends. In our case, we can write the j-th basis function as follows:

$$B_j(\mathbf{l}) = \prod_{m=1}^{M_j} b_{m,j}(\mathbf{l}), \tag{18}$$

where M_j is the number of univariate hinge functions $b_{m,j}$. We can write the MARS model for the expected recourse function accordingly:

$$\hat{Q}(\mathbf{l}) = \sum_{j=0}^{J} a_j B_j(\mathbf{l}), \tag{19}$$

where a_j is the coefficient of the j-th basis function.

3.4 Optimization of the Approximated S-UCED Model

The last step in the DACE approach is to optimize the resulting model, which consists of the first stage cost function as well as the MARS approximation $\hat{Q}(\mathbf{l})$ for the second stage.

$$\begin{aligned} \min \ & f(\mathbf{u},\mathbf{v}) := c^\top[\mathbf{u};\mathbf{v}] + \hat{Q}(\mathbf{l}) \\ \text{s.t } & (\mathbf{u},\mathbf{v}) \in \mathcal{V} := \{(\mathbf{u},\mathbf{v}) \mid A[\mathbf{u};\mathbf{v}] = b\} \subseteq \mathbb{B}^{m_1} \times \mathbb{R}_+^{n_1}, \\ & \mathbf{u} = (\mathbf{x},\mathbf{s},\mathbf{z}), \\ & l_{gi} = \sum_{t \in \mathcal{T}_i} x_{g,h} \qquad \forall g \in \mathcal{G} \qquad \forall i \in \mathcal{I}. \end{aligned} \tag{20}$$

It can be shown that if $\hat{Q}(\mathbf{l})$ is constructed using non-smooth and two-way interaction truncated linear (TITL) form of the MARS function, it can be formulated as a mixed-integer quadratic programming (MIQP) model and therefore, globally optimized. For a full description of using MIQP to formulate $\hat{Q}(\mathbf{l})$, we refer the interested reader to Ju et al. [2022].

3.5 Solution Quality Assessment

Let us revisit the S-UCED problem in (14). For computational tractability, the expectation in the objective function is often replaced by a sample average computed using a set of random scenarios $\Xi_{n'} \subseteq \Xi$ of demand and renewable generation. Here, n' is the size of the random sample. The resulting problem is the SAA of the S-UCED and is written as

$$f_{n'}(\mathbf{u},\mathbf{v}) = \min_{(\mathbf{u},\mathbf{v}) \in \mathcal{V}} \big\{ c(\mathbf{u},\mathbf{v}) + \frac{1}{n'} \sum_{i=1}^{n'} Q(\mathbf{u},\xi_i) \big\}. \tag{21}$$

We denote the optimal value of the true 2-SP and the SAA by a^* and $a^*_{n'}$, respectively.

Since the sample is generated randomly, the resulting solutions and values are stochastic in nature. Therefore, it is necessary to assess the quality of the solutions obtained from the optimization process. Mak et al. [1999] introduced a multiple replication-based procedure for assessing the quality of solutions obtained from the a sampling-based approach. In an M-replicated procedure, we generate M samples of independent identically distributed (iid)

observations $\{\xi_1^m, \xi_2^m, ..., \xi_{n'}^m\}$, each of size n'. We construct and solve (21) to obtain $a_{n'}^{*,m}$ and $(\mathbf{u}_{n'}^{*,m}, \mathbf{v}_{n'}^{*,m})$. An estimate of $\mathbb{E}\{a_{n'}^*\}$ which is a lower bound for the true optimal value a^* can be estimated by $\mathcal{L}_{n'}$, given by

$$\mathcal{L}_{n'} = \frac{1}{M} \sum_{m=1}^{M} a_{n'}^{*,m}. \tag{22}$$

The upper bound, $\mathbb{E}\{f(\hat{\mathbf{u}}, \hat{\mathbf{v}})\}$ with a suboptimal solution $(\hat{\mathbf{u}}, \hat{\mathbf{v}})$, can be estimated using an evaluation sample of size n'' iid observations $\{\xi_1^m, \xi_2^m, ..., \xi_{n''}^m\}$ simulated independently of the optimization set of n' scenarios. In particular, for $\mathbf{u}_{n'}^{*,m}, \mathbf{v}_{n'}^{*,m}$ at the m-th replication we have

$$\mathcal{U}_{n''}^m = c(\mathbf{u}_{n'}^{*,m}, \mathbf{v}_{n'}^{*,m}) + \frac{1}{n''} \sum_{i=1}^{n''} Q(\mathbf{u}_{n'}^{*,m}, \mathbf{v}_{n'}^{*,m}, \xi_j^m). \tag{23}$$

It is preferred that the evaluation sample size be significantly higher than the optimization sample size, i.e, $n'' \gg n'$. For M replications, the upper bound estimate can be immediately computed as

$$\mathcal{U}_{n''} = \frac{1}{M} \sum_{m=1}^{M} \mathcal{U}_{n''}^m. \tag{24}$$

Let $\sigma_{\mathcal{L}}^2$ and $\sigma_{\mathcal{U}}^2$ be the standard sample variance of $\mathcal{L}_{n'}$ and $\mathcal{U}_{n''}$, respectively. We can compute a $(1-\alpha)$-confidence interval (CI) on the lower bound and the upper bound estimates as:

$$\mathrm{CI}_{\mathcal{L}} = \big[\mathcal{L}_{n'} \pm \frac{\zeta_{a/2}\sigma_{\mathcal{L}}}{\sqrt{M}}\big]; \quad \mathrm{CI}_{\mathcal{U}} = \big[\mathcal{U}_{n''} \pm \frac{\zeta_{a/2}\sigma_{\mathcal{U}}}{\sqrt{M}}\big], \tag{25}$$

where $\zeta_{a/2}$ is the $(1-a/2)$ quantile of the standard normal distribution. We can define the worst-case optimality gap, which we refer to as the *pessimistic gap*, as the difference between the upper end of $CI_{\mathcal{U}}$ and the lower end of the $CI_{\mathcal{L}}$. If the pessimistic gap is acceptably smaller than a threshold, then the SAA procedure is terminated with a statistical guarantee on the optimal objective value.

4 Numerical Results

For our case study, we conduct experiments on a modified IEEE118 bus system. This test system has 54 generators of which 36 are conventional, and the remaining 18 are renewable

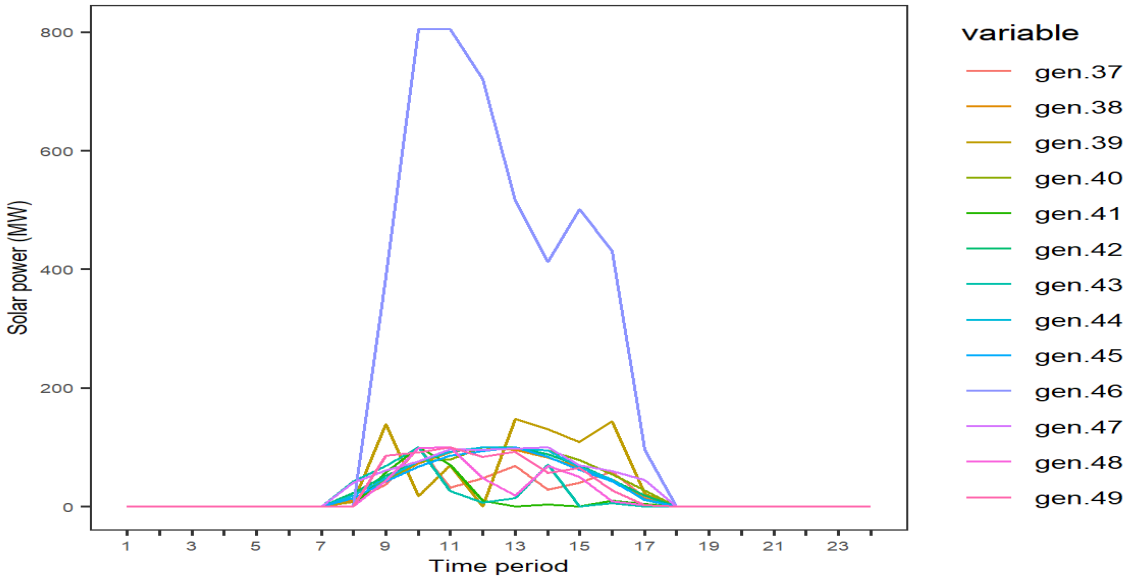

Figure 3: Power at solar generators vs time

(wind and solar) generators. The scenarios of wind and solar generation are based on a sample of size $n = 1000$ simulated in the R platform using a time series model. The LHS algorithm as well as fitting the MARS model are also performed in R. The optimization procedures are conducted on a $C/C++$ platform with CPLEX 12.9 as the solver on a Linux-based server with a processor of 64 GB RAM.

The original $\mathbf{x}$ space contains 2592 features, which represent the 36 conventional generators over the 24-hour planning horizon. For the dimension of the $\mathbf{l}$ variables, we observe the patterns at the energy output of the simulated time series for different renewable generators that have a direct impact on whether conventional generators have to be operational or renewable units are adequate to meet the demand at that certain time period t. As illustrated in Figure 3, solar power forecasts demonstrate a pattern of zero from time period $t = 1$ to $t = 7$. The peak of solar power is shown to be between $t = 8$ and $t = 17$ and finally from $t = 18$ to $t = 24$, we observe zero power once more. Based on these patterns, we set $\mathcal{I} = 3$ at different time lengths of $|\mathcal{T}_1| = 7$, $|\mathcal{T}_2| = 10$ and $|\mathcal{T}_3| = 7$ for each generator g. This results in 108 features for the $\mathbf{l}$ space. Specifically, the dimensionality reduction procedure allows the implementation of the LHS algorithm on 108 features instead of the original 2592 decision values.

4.1 DoE Procedure

In order to implement Algorithm 1, we consider $2 \times \Omega_g = 6$ as the overall number of remain-on and remain-off time periods.

For the commitment linking space with 108 features, we initially consider $n = 300$ observations in the DoE process. Eliminating the observations that represented infeasible first-stage solutions leaves us with 205 feasible design points. Once the sampled commitment decisions are obtained via the experimental design, we conduct the experiments in the following sections with $M = 30$ replicated scenarios of sample size $n' = 1000$.

4.2 Optimization of the Expected Recourse Function

The second-stage problem (14b) is solved using $n' = 1000$ generated random scenarios using the 205 sampled design points as first-stage solutions. The expected recourse function is estimated to be the average of the second-stage recourse value over these scenarios.

4.3 MARS Models

We use the `earth` package in *R* to conduct the MARS algorithm in order to predict the expected recourse function. In our procedure, we observe that the replications merely differ in the interaction terms and not the main effects. Figure 4 illustrates the number of interaction terms for the 30 replicated MARS models. While the average R-squared remains around 0.98 across the replications, the number of interaction terms varies between 13 and

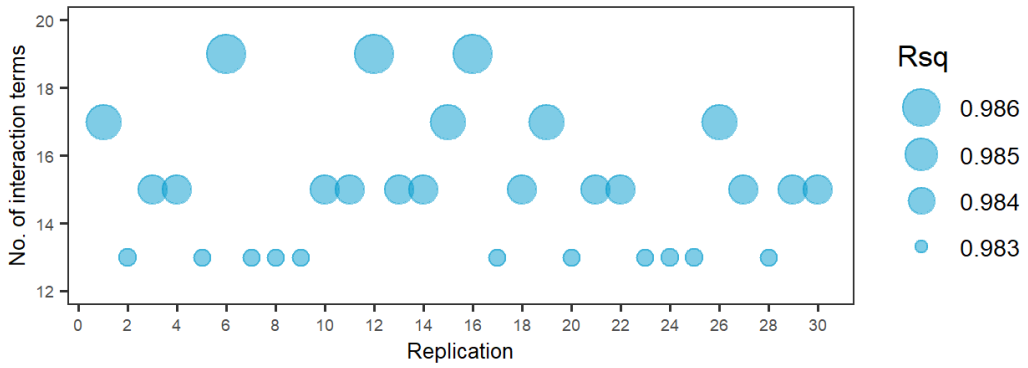

Figure 4: Number of interaction terms for 30 replicated MARS models

19. The MARS procedure automatically chooses which variables are the most important ones to use, the positions of the knots in the hinge functions, and how the univariate hinge functions are combined.

These 30 MARS models help us gain information about how the committed generators impact the operating costs as raised in the contribution. In particular, Figure 5 captures the solutions predicted by the first replicated MARS model at different time periods in the 24-hour horizon. This Figure suggests that a lot of the conventional generators remain offline in the second part of the day ($\mathcal{T}_2$) in the presence of *renewable energy* and online in

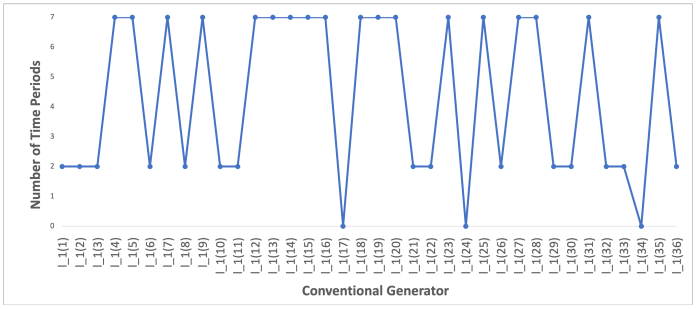

(a) Conventional generator operational time for $\mathcal{T}_1$

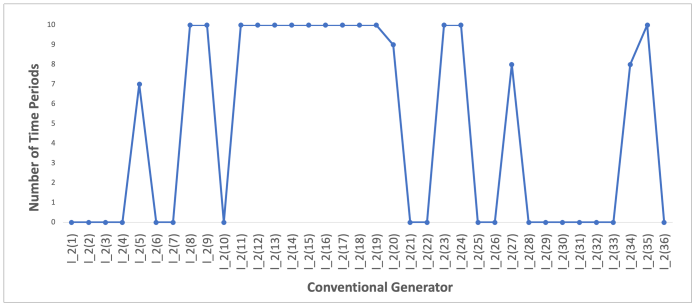

(b) Conventional generator operational time for $\mathcal{T}_2$

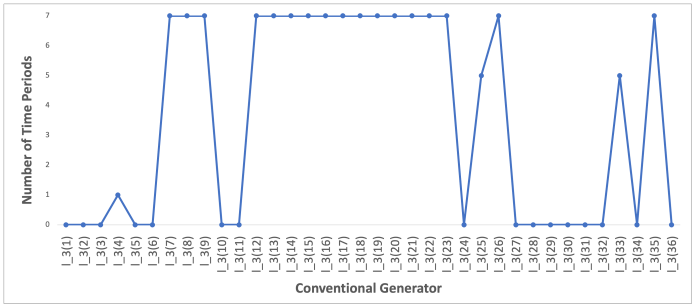

(c) Conventional generator operational time for $\mathcal{T}_3$

Figure 5: Operational status of the conventional generators for replication 1 in the three time parts of the day

the first and third parts of the day ($\mathcal{T}_1$ and $\mathcal{T}_3$) to compensate for the absence of renewable generation as seen previously in Figure 3 for the same replication. Let us consider generator 25 as an example. For this particular generator, the interaction terms of the first replicated MARS model have the following form:

$$1167.52 * \max(0, 6 - l_{7,2}) * \max(0, 5 - l_{25,3}) +$$
$$1464.66 * \max(0, l_{7,2} - 6) * \max(0, 5 - l_{25,3})$$

Moreover, Figure 6 depicts the univariate terms for variables $l_{7,3}$ and $l_{25,3}$ with knots at $k = 6$ and $k = 5$, respectively. Since the objective of the second stage is to minimize the ED problem, the recourse function would be minimized with generators 7 and 25 remaining offline in the third part of the day as shown in the univariate terms in Figure 6. However, in order to fulfill the demand in the second part of day, generator 7 should remain online

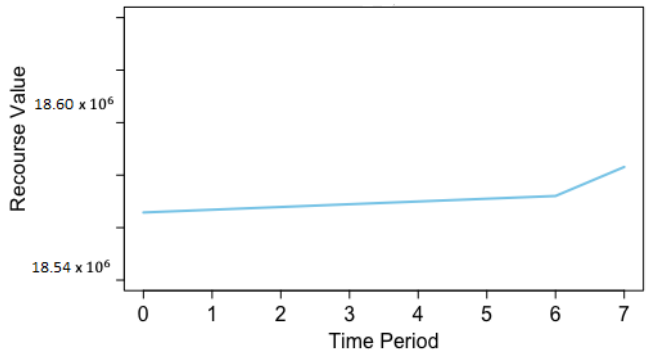

(a) Univariate hinge function for generator 7 at $\mathcal{T}_3$

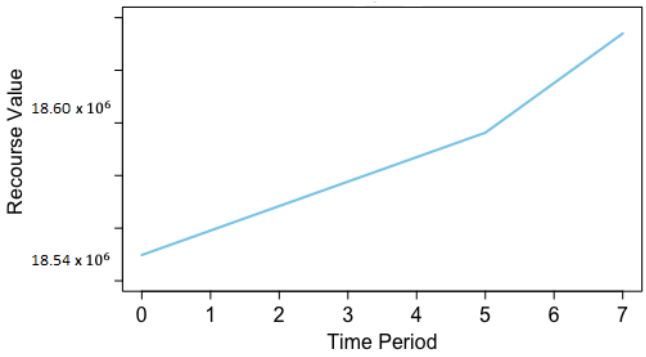

(b) Univariate hinge function for generator 25 at $\mathcal{T}_3$

Figure 6: The univariate terms of generators 7 and 25 in the third part of the day

since the demand decreases as its number of remaining online time periods increases. This is indicated in the first interaction term. However, due to its minimum uptime as well as the shedding penalty restrictions, this generator cannot remain online for more than 6 consecutive time periods. While having generator 25 online for more than 5 hours will reduce the interaction terms, it will increase the expected cost of shedding in the third part of the day due to the large coefficients of the univariate terms. For the plots of the two-way interaction terms at this particular replication, we refer the reader to Appendix A.

4.4 Optimization of the S-UCED Model

Once we obtain the predicted recourse function, we can set $\hat{Q}$ as an approximation to the second stage problem (14b) and alternatively solve (20). Across $M = 30$ replications, we use the resulting optimal solutions as an input to solve the original S-UCED model using (21). This is our lower bound estimate, which we refer to it as the predicted value.

Since (21) has finite support, we can use the L-shaped method to solve the SAA problem. We use the results as a basis of comparison for our DACE-based approach. The SAA instance is solved using a sample size of $n' = 1000$ across the M replicated scenarios terminated at $\epsilon = 0.05$ as the optimality gap. This gap is defined as the difference between the in-sample upper and lower bound within the acceptable tolerance of 0.05 in the L-shaped optimization process. The results of solving the IEEE118 instance with the two methods are summarized in Table 1. This table presents the estimates for the lower bound, $\mathcal{L}_{n'}$, for $n' = 1000$, and the out-of-sample bound, $\mathcal{U}_{n''}$, which we refer to as the validated value for $n'' = 10,000$ along with their standard deviations. Notice that the DACE approach presents a lower objective value than the optimal value using the L-shaped method reported within 5% of optimality. In addition, the solutions obtained from the DACE approach show lower variability compared to the L-shaped solutions. This can be attributed to the fact that the replicated MARS models have low sensitivity toward the 30 replicated scenario sets differing only in the interaction terms as demonstrated in Figure 4. The last column of Table 1 shows the average computational time. This time includes the overall time of executing the steps of the two methods. Notice that the DACE approach significantly reduces the overall computational time compared to the L-shaped method. Moreover, the DACE approach provides more reliable validation results.

Algorithm	Predicted value ($\mathcal{L}_{n'}$) (std.dev.)	Validated value ($\mathcal{U}_{n''}$) (std.dev.)	Avg. time (H:M:S) (std.dev.)
DACE	$ 20,450,610.52 (11,036.67)	$ 20,433,886.61 (11,086.58)	0:19:37.29 (0:0:7.22)
L-shaped	$ 20,500,531.22 (30,572.14)	$ 20,681,876.84 (95,981.80)	6:25:42.25 (5:2:15.84)

Table 1: Results from DACE vs. L-shaped for IEEE118

We report the time results for each step of the DACE and L-shaped procedures in Table 2. Note that in the L-shaped method, solving the subproblems accounts for a considerable portion of the computational time. However, this number decreases significantly when fixing the first stage solutions using our experimental design approach to solve the recourse functions across the DoE points in the DACE procedure.

Step	Description	Avg time (H:M:S) (std.dev.)
`DACE`		
1	Generate LHS using Algorithm 1	0:0:22.21 (0:0:0.00)
2	Generate recourse function values	0:19:13.51(0:0:7.21)
3	Fit a MARS approximation	0:0:0.82 (0:0:0.07)
4	Optimization to obtain the first stage solution	0:0:0.76 (0:0:0.07)
`L-shaped`		
1	Optimization of the Subproblems	5:48:16.96 (4:24:54.67)
2	Optimization of the Master problem	0:32:45.63 (0:35:15.34)

Table 2: Computational Time for the DACE and L-shaped procedures

As depicted in Figure 7, the mean differences of the out-of-sample estimate for the L-shaped method show that the total validated costs can be as high as $20.92 million. However, while demonstrating less variability across the 30 replicated values, the DACE approach suggests that the total validated costs can be at most $20.46 million.

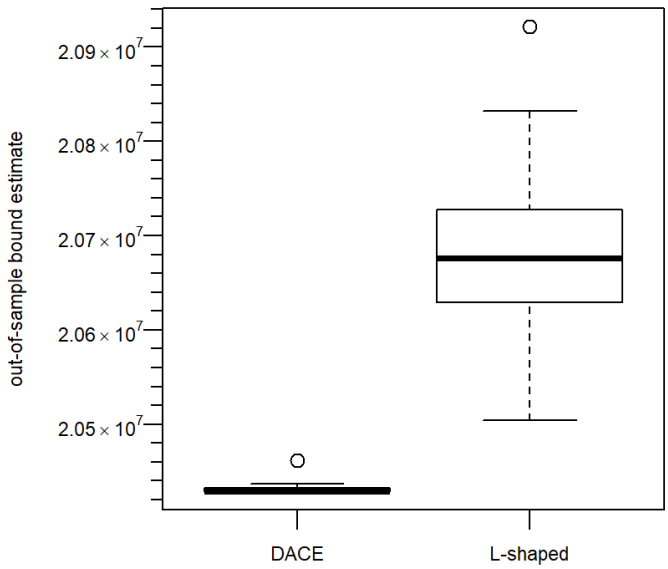

Figure 7: Mean differences of out-of-sample estimate for DACE vs Lshaped

5 Concluding Remarks and Future Work

In this paper, we presented the first application of a DACE-based statistical approach to optimize the S-UCED with uncertainties in renewable generation. We proposed a creative experimental design sampling specifically developed to simulate the first stage decisions and solve the second stage continuous recourse values. We presented a MARS approximation to predict the second-stage recourse function. This approach demonstrates great efficiency in approximating complex functions within optimization. In particular, the computational results on a large-scale (IEEE118) test system verify the significant computational improvement over the conventional L-shaped method where we use a multiple replication procedure to assess the quality of our stochastic solutions obtained from both methods. In addition, as a result of the significant reduction in the computational time of optimizing the SP model, this approach can be used as an alternative method to solve SP problems arising in power systems planning and operations applications within the common dedicated time frame considered in the electricity market. Future work will address additional approaches to tackle the challenge of generating DoE points that violate the valid inequalities in the UC model. The efficient optimization of the MARS approximation with enforced convexity and

using derivatives of the MARS function to generate cuts are also topics of future research.

Utilizing SAA in the optimization process necessitates the selection of the samples *a priori*. Since one subproblem is solved for each scenario, their relative performance is often problem-dependent. This often results in an increase in the computational time by increasing the sample size. Sequential sampling algorithms such as the SD method [Higle and Sen, 1991] have been prevalent in tackling this issue. SD uses a sequence of approximations built by introducing new scenarios in every iteration. However, the SD method cannot handle discrete variables in the first stage. A development of a customized SD method is a subject for future work. Other approaches such as a decomposition method across scenarios in addition to the time periods can provide more information about the status of the generator when solving problems with varying scenarios. In our future research, we will investigate improvements to address these challenges in solving S-UCED models.

References

Bob Perciasepe. *The clean-energy transition is powering the U.S. economy*, 2017. URL `https://www.c2es.org/2017/04/the-clean-energy-transition-is-powering-the-u-s-economy/`.

C2ES. *Renewable Energy*, 2018. URL `https://www.c2es.org/content/renewable-energy/`.

EIA. *Renewable Energy Standards*, 2019. URL `https://www.eia.gov/energyexplained/renewable-sources/portfolio-standards.php`.

Alireza Fallahi, Jay M Rosenberger, Victoria CP Chen, Wei-Jen Lee, and Shouyi Wang. Linear programming for multi-agent demand response. *IEEE Access*, 7:181479–181490, 2019a.

Alireza Fallahi et al. *A MULTI-AGENT DEMAND RESPONSE PLANNING AND OPERATIONAL OPTIMIZATION FRAMEWORK*. PhD thesis, 2019b.

Alireza Fallahi, Jay M Rosenberger, Victoria CP Chen, Wei-Jen Lee, and Shouyi Wang. Stochastic bounds on real-time multi-agent demand response. 2020. URL `https://cosmos.uta.edu/technical-reports/`.

Semih Atakan, Harsha Gangammanavar, and Suvrajeet Sen. Towards a sustainable power grid: Stochastic hierarchical planning for high renewable integration, 2021.

GJ Osório, JM Lujano-Rojas, JCO Matias, and JPS Catalão. A probabilistic approach to solve the economic dispatch problem with intermittent renewable energy sources. *Energy*, 82:949–959, 2015.

Rolf Wiebking. Stochastische modelle zur optimalen lastverteilung in einem kraftwerksverbund. *Zeitschrift für Operations Research*, 21(6):B197–B217, 1977.

Samer Takriti, John R Birge, and Erik Long. A stochastic model for the unit commitment problem. *IEEE Transactions on Power Systems*, 11(3):1497–1508, 1996.

R Tyrrell Rockafellar and Roger J-B Wets. Scenarios and policy aggregation in optimization under uncertainty. *Mathematics of operations research*, 16(1):119–147, 1991.

Pierre Carpentier, Guy Gohen, J-C Culioli, and Arnaud Renaud. Stochastic optimization of unit commitment: a new decomposition framework. *IEEE Transactions on Power Systems*, 11(2):1067–1073, 1996.

Takayuki Shiina and John R Birge. Stochastic unit commitment problem. *International Transactions in Operational Research*, 11(1):19–32, 2004.

Jianhui Wang, Mohammad Shahidehpour, and Zuyi Li. Security-constrained unit commitment with volatile wind power generation. *IEEE Transactions on Power Systems*, 23(3): 1319–1327, 2008.

Ruiwei Jiang, Muhong Zhang, Guang Li, and Yongpei Guan. Two-stage robust power grid optimization problem. *submitted to Journal of Operations Research*, pages 1–34, 2010.

Dimitris Bertsimas, Eugene Litvinov, Xu Andy Sun, Jinye Zhao, and Tongxin Zheng. Adaptive robust optimization for the security constrained unit commitment problem. *IEEE transactions on power systems*, 28(1):52–63, 2012.

Qipeng P Zheng, Jianhui Wang, and Andrew L Liu. Stochastic optimization for unit commitment—a review. *IEEE Transactions on Power Systems*, 30(4):1913–1924, 2014.

K Liu and J Zhong. Generation dispatch considering wind energy and system reliability. In *IEEE PES General Meeting*, pages 1–7. IEEE, 2010.

John Hetzer, C Yu David, and Kalu Bhattarai. An economic dispatch model incorporating wind power. *IEEE Transactions on energy conversion*, 23(2):603–611, 2008.

Harsha Gangammanavar, Suvrajeet Sen, and Victor M Zavala. Stochastic optimization of sub-hourly economic dispatch with wind energy. *IEEE Transactions on Power Systems*, 31(2):949–959, 2015.

Francois Bouffard and Francisco D Galiana. Stochastic security for operations planning with significant wind power generation. In *2008 IEEE Power and Energy Society General Meeting-Conversion and Delivery of Electrical Energy in the 21st Century*, pages 1–11. IEEE, 2008.

Jianhui Wang, Audun Botterud, Vladimiro Miranda, Cláudio Monteiro, and Gerald Sheble. Impact of wind power forecasting on unit commitment and dispatch. In *Proc. 8th Int. Workshop Large-Scale Integration of Wind Power into Power Systems*, pages 1–8, 2009.

A Papavasiliou and S.S. Oren. Multiarea stochastic unit commitment for high wind penetration in a transmission constrained network. *Operations Research*, 61(3):578–592, 2013. doi: 10.1287/opre.2013.1174. URL `http://dx.doi.org/10.1287/opre.2013.1174`.

Nahal Sakhavand and Harsha Gangammanavar. Subproblem sampling-based stochastic programming method for power systems planning and operations problems. 2020. URL `https://people.smu.edu/harsha/files/2020/10/Sakhavand_Gangammanavar_stocUCED.pdf`.

Richard M Van Slyke and Roger Wets. L-shaped linear programs with applications to optimal control and stochastic programming. *SIAM Journal on Applied Mathematics*, 17 (4):638–663, 1969.

A. Shapiro, D. Dentcheva, and A. Ruszczynski. *Lectures on Stochastic Programming: Modeling and Theory, Second Edition*. Society for Industrial and Applied Mathematics, Philadelphia, PA, USA, 2014. ISBN 1611973422, 9781611973426.

Qianfan Wang, Yongpei Guan, and Jianhui Wang. A chance-constrained two-stage stochastic program for unit commitment with uncertain wind power output. *IEEE Transactions on Power Systems*, 27(1):206–215, 2011.

Yang Liu and Nirmal-Kumar C Nair. A two-stage stochastic dynamic economic dispatch model considering wind uncertainty. *IEEE Transactions on Sustainable Energy*, 7(2): 819–829, 2015.

Kwok Cheung, Dinakar Gade, César Silva-Monroy, Sarah M Ryan, Jean-Paul Watson, Roger J-B Wets, and David L Woodruff. Toward scalable stochastic unit commitment. *Energy Systems*, 6(3):417–438, 2015.

Jerome Sacks, William J Welch, Toby J Mitchell, and Henry P Wynn. Design and analysis of computer experiments. *Statistical science*, pages 409–423, 1989.

VCP Chen. Measuring the goodness of orthogonal array discretizations for stochastic programming and stochastic dynamic programming. *SIAM Journal on Optimization*, 12: 322–344, 01 2001.

Venkata L. Pilla, Jay M. Rosenberger, Victoria C. P. Chen, and Barry Smith. A statistical computer experiments approach to airline fleet assignment. *IIE Transactions*, 40(5): 524–537, 2008. doi: 10.1080/07408170701759734. URL `https://doi.org/10.1080/07408170701759734`.

Venkata L Pilla, Jay M Rosenberger, Victoria Chen, Narakorn Engsuwan, and Sheela Siddappa. A multivariate adaptive regression splines cutting plane approach for solving a two-stage stochastic programming fleet assignment model. *European Journal of Operational Research*, 216(1):162–171, 2012.

Dennis KJ Lin, Timothy W Simpson, and Wei Chen. Sampling strategies for computer experiments: design and analysis. *International Journal of Reliability and applications*, 2(3):209–240, 2001.

HD Patterson. The errors of lattice sampling. *Journal of the Royal Statistical Society: Series B (Methodological)*, 16(1):140–149, 1954.

Michael D McKay, Richard J Beckman, and William J Conover. A comparison of three methods for selecting values of input variables in the analysis of output from a computer code. *Technometrics*, 42(1):55–61, 2000.

Jerome H Friedman. Multivariate adaptive regression splines. *The annals of statistics*, pages 1–67, 1991.

Victoria CP Chen, Kwok-Leung Tsui, Russell R Barton, and Martin Meckesheimer. A review on design, modeling and applications of computer experiments. *IIE transactions*, 38(4):273–291, 2006.

Semih Atakan, Guglielmo Lulli, and Suvrajeet Sen. A state transition mip formulation for the unit commitment problem. *IEEE Transactions on Power Systems*, 33(1):736–748, 2017.

Michael Kutner, Christopher Nachtsheim, and John Neter. *Applied Linear Regression Model*, volume 26. 01 2004. doi: 10.2307/1269508.

Bancha Ariyajunya, Ying Chen, Victoria Chen, Sb Kim, and Jay Rosenberger. Addressing state space multicollinearity in solving an ozone pollution dynamic control problem. *European Journal of Operational Research*, 289, 07 2020. doi: 10.1016/j.ejor.2020.07.014.

Xinglong Ju, Jay M. Rosenberger, Victoria C. P. Chen, and Feng Liu. Global optimization on non-convex two-way interaction truncated linear multivariate adaptive regression splines using mixed integer quadratic programming. *Information Sciences*, 597(1): 38–52, 2022. ISSN 0020-0255. doi: https://doi.org/10.1016/j.ins.2022.03.041. URL `https://www.sciencedirect.com/science/article/pii/S002002552200250X`.

Wai-Kei Mak, David P Morton, and R Kevin Wood. Monte carlo bounding techniques for determining solution quality in stochastic programs. *Operations research letters*, 24(1-2): 47–56, 1999.

J. L. Higle and S Sen. Stochastic decomposition: An algorithm for two-stage linear programs with recourse. *Mathematics of Operations Research*, 16(3):650–669, 1991. ISSN 0364765X.

A MARS Interaction Terms

Each graph in Figure 8 shows the interaction terms in the MARS model between two predictor variables at different periods of the day. For example, we observe the predicted value of Q, as $l_{27,2}$ and $l_{27,3}$ vary, with other variables fixed at their median values.

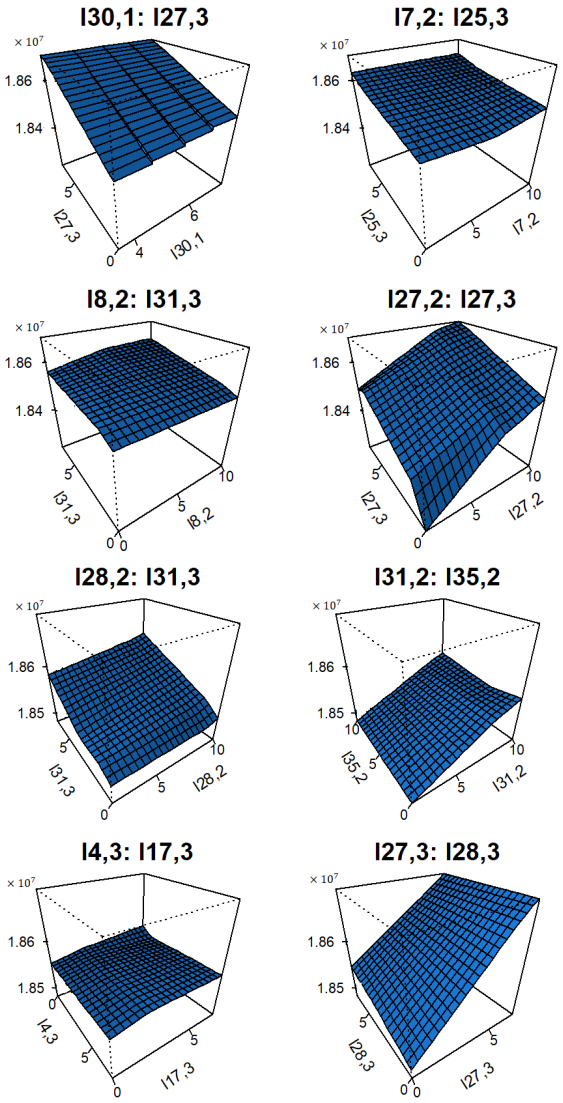

Figure 8: Interaction terms in the MARS model